Mechanisms underlying strong-field double ionization of argon dimers

B. Manschwetus,[1] H. Rottke,[1] G. Steinmeyer,[1] L. Foucar,[2] A. Czasch,[3] H. Schmidt-Böcking,[3] and W. Sandner[1]

[1]*Max-Born-Institut, Max-Born-Strasse 2A, D-12489 Berlin, Germany*

[2]*Max Planck Advanced Study Group, Center for Free Electron Laser Science, Notkestrasse 85, D-22607 Hamburg, Germany*

[3]*Institut für Kernphysik, Goethe Universität Frankfurt, Max-von-Laue-Strasse 1, D-60438 Frankfurt, Germany*

(Received 12 April 2010; published 19 July 2010)

We investigate double ionization of argon dimers in high-intensity ultrashort Ti:sapphire laser pulses. We are able to identify several strong-field excitation pathways of the dimer that terminate in atomic ion pairs from a Coulomb explosion. The explosion starts from two-site double-ionized dimers and from one-site double-ionized ones after radiative charge transfer at small internuclear separation. One-site double ionization is accomplished by laser-induced charge transfer in the high-intensity laser pulse following two-site double ionization. The highest energy ion pairs we observed can be attributed to "frustrated triple ionization" of the argon dimer.

DOI: 10.1103/PhysRevA.82.013413 PACS number(s): 33.80.Rv, 33.80.Wz

I. INTRODUCTION

Noble gas dimers are bound by weak polarization forces at a substantially larger internuclear separation than ordinary molecules. This gives rise to a localization of the electrons at the two atomic centers. Photoionization of these species in a high-intensity laser pulse is expected to proceed in a different way than strong-field ionization of strongly bound molecules with delocalized valence electrons. Moreover, processes induced in the ion are possibly not necessarily found after photoionization of electrons from delocalized molecular orbitals. Single ionization of one of the constituent atoms may, for example, start electron charge oscillations between the singly charged ion and the neighboring atom. Charge transfer, which is induced by fast electronic charge migration, presumably also plays a significant role in larger organic molecules after local ionization of a chromophore [1–3]. In large argon clusters it is assumed to be the origin of regular structures in the velocity distribution of charged fragments which have been observed after ionizing them with high-intensity ultrashort laser pulses [4]. Strong-field double ionization of a dimer may be induced by locally removing either one electron at each atomic site or two at a single site with the following ionic decay being completely different. Alternatively, two-site double ionization may be followed by a laser-induced charge transfer, which finally again results in one-site double ionization. Despite the expected new phenomena only a few strong-field ionization experiments have been done to date, specifically with noble gas dimers that may be viewed as model systems for molecules at large internuclear separation in general and possibly for larger molecules with isolated excitation centers [5].

Here we investigate the double ionization (DI) mechanisms of Ar_2 dimers and the fragmentation dynamics of Ar_2^{2+} in ultrashort high-intensity laser pulses. This elementary unit is assumed to be the origin of a specific cluster dissociation which was observed in [4] after strong-field excitation. We specifically focus on Coulomb explosion. We choose a laser pulse width which prevents nuclear motion while the pulse is being applied. Consequently, excitation energy input and nuclear dynamics are well separated in time. At first sight, one therefore might expect to find basically a Coulomb explosion after two-site DI that starts at the equilibrium internuclear separation R_{eq} of the neutral Ar_2 dimer. However, besides this obvious channel we find Ar^+ ion pairs with a substantially higher kinetic energy release. One way to gain this energy would be a Coulomb explosion starting at a considerably smaller internuclear separation. Such a small separation can, however, only be reached provided that the light pulse initially doubly ionizes the dimer at one site (Ar^{2+}-Ar) or that one-site singly charged and excited ions (Ar^{+*}-Ar) are formed, which may decay via "interatomic Coulombic decay" (ICD) [6–9]. A third mechanism for high kinetic energy gain directly at R_{eq} without the necessity for a closer approach of the nuclei would be "frustrated triple ionization", where Ar_2 is left doubly ionized after the laser pulse has passed by, however, with one electron caught in a high Rydberg state of the triply charged Ar_2^{3+} ion core [10,11].

II. EXPERIMENT

In the experiment we use Ti:sapphire laser pulses (wavelength, 800 nm) with a width of 25 fs at a repetition rate of 3 kHz. The laser beam is focused into a COLTRIMS (cold target recoil ion momentum spectroscopy) setup [12] using a spherical mirror with a focal length of 150 mm. With laser pulse energies of $\approx$14 μJ we reach light intensities in the focal spot that are close to the threshold for saturation of single ionization of atomic argon ($\approx 3 \times 10^{14}$ W/cm^2). The state of polarization and the direction of linear polarization of the light beam are adjusted by a quarter-wave plate and a half-wave plate, respectively.

Ar_2 dimers are formed by supersonic expansion of argon gas. The supersonic beam, which contains a small fraction of dimers ($\approx$2%), is intersected by the laser beam in its focal spot [13]. Ions are extracted from the interaction region by a homogeneous electric field (field strength, 3020 V/m). After acceleration and free drift they impinge on a multichannel plate detector equipped with a position-sensitive anode. For each detected ion the time of flight and the impact position on the detector are recorded. This permits the reconstruction of its momentum vector. The Coulomb explosion channel of Ar_2 is filtered out by triggering the data acquisition only by ion pair events. Additionally, in the following data analysis false ion pair events that do not obey momentum conservation are

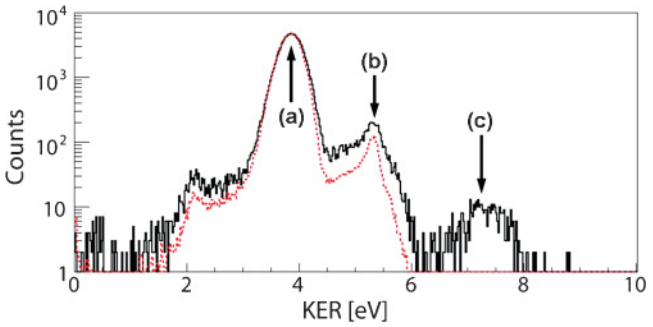

FIG. 1. (Color online) The ion pair KER after strong-field double ionization of argon dimers at a laser pulse peak electric-field strength of 0.1 a.u. Solid (black) line, linear polarization; dashed (red) line, circular polarization of the laser beam.

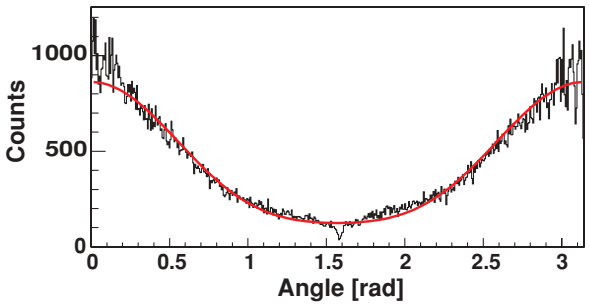

FIG. 2. (Color online) Angular distribution of the ion pair from DI of Ar_2 for the KER line (a) in Fig. 1 (the direct Coulomb explosion line) for linearly polarized laser radiation. Plotted is the number of events per solid angle element $d\Omega = 2\pi \cos\theta d\theta$ as a function of θ, the angle between the laser beam polarization axis and the direction of emission of one of the Ar^+ ions. For direct Coulomb explosion this angle is equal to the angle between the light polarization axis and the internuclear axis of the dimer at the instant of ionization. The laser pulse parameters are those of Fig. 1.

removed. This eliminates accidental double hits and possible Ar^+ double hits after multiple ionization of larger clusters that are also present in the beam, however, at a smaller concentration than dimers.

III. RESULTS AND DISCUSSION

Figure 1 shows the kinetic energy release (KER) distribution of Ar^+ ion pairs emerging from strong-field DI of Ar_2 dimers on a logarithmic number of events scale to display all relevant contributions in the energy range from 0 to 10 eV. Two traces are shown, one for linear polarization of the laser beam [solid (black) line] and one for circular polarization [dashed (red) line]. The light intensity was chosen to be $I_{\rm lin} = 3.1 \times 10^{14}$ W/cm^2 and $I_{\rm circ} = 2I_{\rm lin}$ for linear and circular polarization, respectively. This choice ensures equal electric-field strength amplitudes for both polarization states. The number of events is adjusted to the same value at the maximum of the main KER line at 3.85 eV [line (a)]. Two further lines [(b) and (c)] are found in the spectrum at 5.3 eV and at 7.3 eV with line (c) being very weak. Below 2.6 eV events prevail that do not stem from dissociation of Ar_2^{2+} ions. The main contribution to the spectrum here most likely originates from dissociation of doubly charged argon trimers ($Ar_3^{2+} \longrightarrow Ar^+ + Ar^+ + Ar$) from a linear conformation (Ar^+-Ar-Ar^+). Similar to Coulomb explosion of Ar_2^{2+} the ion momentum sum for this reaction is also small. These events, thus, cannot be suppressed efficiently by using momentum conservation and contribute to the KER spectrum in Fig. 1. Switching from linear to circular polarization while keeping the electric-field strength fixed results in a slight decrease of line (b) with respect to line (a). Part of this decrease has to be attributed to an increased loss of Ar^+ ions for circular polarization (they miss the multichannel plate detector). The high-energy line (c) completely disappears for circular polarization. This behavior already suggests individual DI mechanisms behind each of the KER lines.

A. Two-site double ionization of Ar_2 [line (a)]

The lowest energy DI threshold $I_p^{2+}(Ar_2)$ of Ar_2 corresponds to the two-site doubly ionized configuration $Ar^+(3p^{-1})$-$Ar^+(3p^{-1})$ where one electron is removed from the $3p$ shell of each atom. The corresponding ionization potential is approximately given by $I_p^{2+}(Ar_2) \approx 2I_p^+(Ar) + 1/R_{\rm eq}$ (atomic units assumed), with $R_{\rm eq}$ being the equilibrium internuclear separation of the Ar_2 dimer ($R_{\rm eq} = 7.13$ a.u. [14]) and $I_p^+(Ar) = 15.76$ eV the ionization potential of atomic argon. $I_p^{2+}(Ar_2)$ amounts to 35.3 eV. The actual lowest energy potential energy curves of Ar_2^{2+} are closely grouped around the simplified Coulomb curve $V_C(R) = 2I_p^+(Ar) + 1/R$ for internuclear separations larger than $R = 5$ a.u. [15]. Based on $V_C(R)$, Coulomb explosion of the two-site ionized dimer at $R_{\rm eq}$ gives rise to a KER ($1/R_{\rm eq}$) of 3.82 eV. This value agrees with the KER of the main line (a) in Fig. 1. The angular distribution of the ion pairs for this line shows a pronounced anisotropy for linearly polarized light with preferred Ar^+ emission along the direction of polarization (see Fig. 2). This means that the double-ionization probability of dimers with the internuclear axis aligned parallel to the laser beam polarization is substantially higher than that for those with the axis aligned perpendicular. An active alignment of Ar_2, however, does not occur; the laser pulse is too short to accomplish this. Two-site Ar_2 DI is thus not equivalent to the ionization of two independent individual atoms as one might have expected at first sight. The dimer structure of the system matters.

In order to scrutinize the two-site DI mechanism we determined the distribution of one component of the sum momentum of the Ar^+ ion pair. For linear polarization the component parallel to the direction of polarization is chosen and for circular polarization one of the equivalent components in the plane of polarization. The ion sum-momentum distribution is a measure for the sum-momentum distribution of the two photoelectrons, which can provide valuable information on the DI mechanism [16,17]. The sum-momentum distributions [dashed (red) lines] are shown in Fig. 3(a) (linear polarization) and in 3(b) (circular polarization) for the KER line (a) in Fig. 1. We compare them with the Ar^{2+} momentum distribution from DI of atomic argon, which was measured simultaneously (blue/dotted lines). The shape of the distributions for linear polarization strongly indicates that two-site DI of the dimer is mediated by sequential electric-field ionization. This shape is

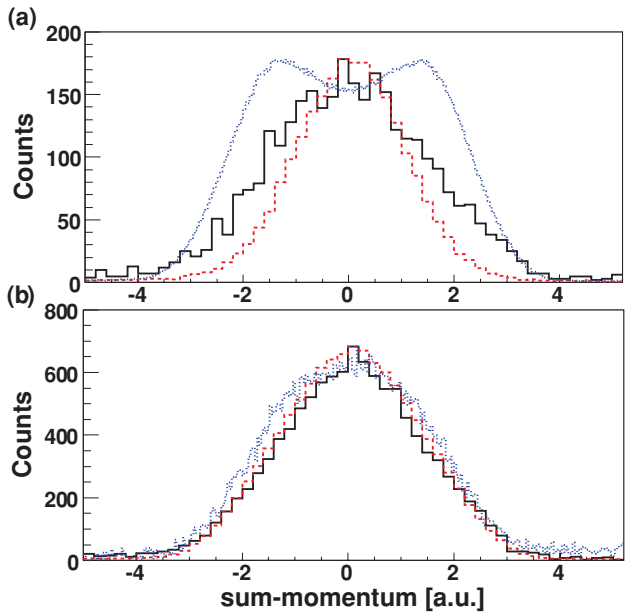

FIG. 3. (Color online) The ion pair sum-momentum distributions for the KER lines (a) [dashed (red) lines] and (b) [solid (black) lines] in Fig. 1. The dotted (blue) lines are the momentum distributions for Ar^{2+} ions from DI of Ar atoms. Part (a) shows the momentum distributions for linear polarization and part (b) shows the momentum distributions for circular polarization of the laser beam. In (a) the momentum component along the direction of linear polarization is displayed and in (b) one of the two equivalent components in the plane of polarization is displayed.

completely different from that of the atomic DI curve. It shows a double-hump structure that is characteristic for nonsequential, electron-impact-induced, double ionization [16,17]. For circular polarization the ion sum-momentum distribution for two-site Ar_2 DI coincides with the momentum distribution of Ar^{2+} ions from atomic DI. Here, in both cases DI is sequential electric-field ionization. Rescattering of the electron that is field ionized in a first step on the singly charged ion core is impossible under these conditions [18].

The preferred two-site DI of dimers aligned along the linear polarization axis of the laser beam (see Fig. 2) by two-step electric-field ionization is suggestive of charge resonance enhanced field ionization of Ar_2^+ in the second step. Ar_2 DI then would resemble, for example, strong-field double ionization of the hydrogen molecule [19–21]. However, there are distinct differences between Ar_2 and H_2 DI: R_{eq} of Ar_2 is from the outset in the range of internuclear separations where charge resonance enhanced ionization has been found in H_2^+ [19–21]. Nuclear dynamics in Ar_2^+ is completely frozen while the laser pulse is applied. Also, for Ar_2^+ two pairs of charge resonance states exist, namely, a $^2\Sigma_{g,u}$ and a $^2\Pi_{g,u}$ pair that are further split by spin-orbit coupling [22]. At R_{eq} the energy separation of the charge resonance pairs is less than ≈0.5 eV [22]. The small energetic separation of the two pairs of states implies that all of them become populated in the first field ionization step of the Ar_2 dimer. This allows charge resonance enhanced ionization to occur in the second ionization step.

B. One-site DI of Ar_2 [line (b)]

A direct two-site DI of Ar_2 cannot give rise to the KER line (b) in Fig. 1, as it would require that the Coulomb explosion start at an internuclear separation considerably smaller than R_{eq}. Also, autoionization of Ar_2^+ ions with a configuration $Ar^+(3p^{-1})$-$Ar(3p^{-1},n\ell)$, where a $3p$ electron of the Ar atom is excited to a state with high principal quantum number n and angular momentum ℓ, cannot generate ion pairs with a KER this high. In these repulsive electronic states [23] the nuclear kinetic energy after single ionization of Ar_2, which is identical to the kinetic energy in the dimer ground state (i.e., a few meV), is much too small to allow a closer approach before autoionization to a two-site ionized Ar_2^{2+} state. The only energetically low-lying Ar_2^+ or Ar_2^{2+} states that may be considered as precursors of the high-energy ion pair dissociation channels we observed are either $Ar^{2+}(3p^{-2})$-Ar one-site doubly ionized or $Ar^+(3p^{-2},n\ell)$-Ar one-site singly ionized and excited configurations (the atomic constituent of the dimer ion is in the ground state). $Ar^+(3p^{-2},n\ell)$-Ar states are lying above the Ar_2 DI threshold as long as the excitation energy in the ion is larger than the ionization threshold of the neutral Ar constituent of the dimer plus the Coulomb repulsion energy of the two nuclei. These states may autoionize at small internuclear separation terminating in a two-site doubly ionized $Ar^+(3p^{-1})$-$Ar^+(3p^{-1})$ state.

The threshold for one-site DI of Ar_2 is similar to that for the atom (i.e., 43.39 eV). One thus expects that at the light intensity used here, Ar_2 one-site DI should be mainly nonsequential like it is in the atom for linearly polarized laser radiation. Consequently, the sum-momentum distribution for the Ar^+ ion pair should be similar to the Ar^{2+} momentum distribution from atomic Ar DI. This, however, is not the case. The corresponding sum-momentum distribution in Fig. 3(a) [solid (black) line] is close to that for two-site DI (red/dashed line), though distinctly broader. It does not show the pronounced double-hump structure typical for nonsequential double ionization. This is strong evidence for nonsequential one-site DI of Ar_2 not being the ionization mechanism behind the KER line (b) in Fig. 1. Two further obvious possibilities remain. One is via one-site singly ionized and excited states $Ar^+(3p^{-2},n\ell)$-Ar. The other is a stepwise mechanism where two-site double ionization is followed by a laser-induced charge transfer in the two-site doubly ionized dimer at R_{eq}.

Unlike the potential energy curves for two-site DI, those for one-site DI configurations are weakly attractive at R_{eq} [15,24] (see Fig. 4). The polarization force exerted on the neutral constituent of the dimer ion by the doubly charged atomic ion is responsible for the attraction. The potential energy of the corresponding electronic states has a minimum around $R \approx 5.2$–5.9 a.u. [15,24]. We expect to find a similar behavior for Ar_2^+ states with an excited Rydberg configuration $Ar^+(3p^{-2},n\ell)$-Ar at least as long as the "orbit" of the Rydberg electron is larger than R_{eq}. All of these electronic states are prone to ICD at all internuclear separations R where their potential energy lies above the threshold for two-site DI to $Ar^+(3p^{-1})$-$Ar^+(3p^{-1})$. Two kinds of ICD mechanisms are known and have been observed experimentally for noble gas dimers: virtual photon exchange also termed "direct contribution" [8,9,25] and, up to now found only for the

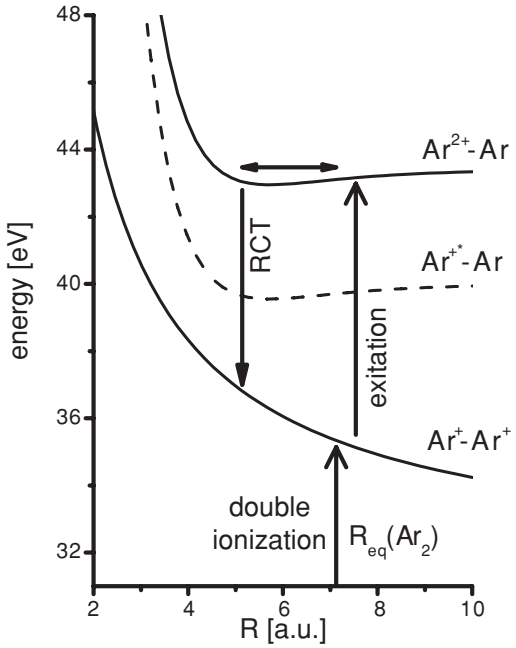

FIG. 4. Schematic potential energy curves of Ar_2^{2+} and Ar_2^{+} relevant for the discussion of the experimental results. The vertical arrows indicate laser-induced DI of Ar_2 and charge transfer in Ar_2^{2+} at the equilibrium internuclear separation R_{eq} of the Ar_2 dimer. The arrow labeled "RCT" indicates reverse radiative charge transfer happening at small internuclear separation.

Ne_2 dimer, radiationless electron exchange (charge transfer) from the Ne atom to one of the $2p$ vacancies in the Ne^+ ion accompanied by ejection of the excited $n\ell$ electron [9,25]. This second mechanism is expected to exist also for the Ar_2 dimer with the only difference that now one of the two $3p$ holes in the ionic constituent of the dimer ion is filled. The two ICD mechanisms are shown schematically in Fig. 5(a). Representative potential energy curves for $Ar^+(3p^{-2},n\ell)$-Ar and $Ar^+(3p^{-1})$-$Ar^+(3p^{-1})$ electronic states which would be involved in this ICD mechanism can be found in Fig. 4. For lack of theoretical data of potential energy curves for $Ar^+(3p^{-2},n\ell)$-Ar Rydberg configurations, Fig. 4 basically shows the vertically displaced ground-state potential energy curve of one-site doubly ionized Ar_2 [15]. This potential reveals the expected attractive character of the $Ar^+(3p^{-2},n\ell)$-Ar states.

Coulomb explosion following the virtual photon exchange [see Fig. 5(a)] happens at or very close to R_{eq} where the laser pulse excites the dimer. Provided it is present, it would add to the main KER line (a) (see, for example, the results found for Ne_2 in [9]). This "radiative" mechanism has a considerable probability to happen even at large internuclear separation. Its rate follows an inverse power law ($\propto 1/R^6$) as a function of the internuclear separation R [26]. At R_{eq} the charge transfer ICD channel has a negligible probability of occurring. It, however, increases exponentially with decreasing internuclear separation as the overlap of the $3p$ orbitals of the dimer constituents increases [9,26]. Based on the single-site doubly ionized potential energy curves of [15,24] we estimate that the $Ar^+(3p^{-2},n\ell)$-Ar potentials allow a minimum accessible internuclear separation of $\approx$5 a.u. to occur (see Fig. 4). There the charge transfer probability should reach a maximum. Coulomb explosion following charge transfer and loss of the Rydberg electron close to this R would fit to our observed KER line (b). Since nuclear dynamics is involved, the charge transfer accompanied by ejection of the excited $n\ell$ electron and the following Coulomb explosion would occur long after the laser pulse is gone, that is, in an unperturbed dimer. One would thus expect to find the ejected electron with a kinetic energy in the energy range between 0 eV and $\approx$7 eV. However, the kinetic energy distribution of photoelectrons detected together with Ar^+ ion pairs with a KER of 5.3 eV [line (b)] for circularly polarized laser radiation does not show the expected electrons in this energy range [27]. Ulrich and coworkers [27] found a photoelectron kinetic energy distribution that is very similar to that taken together with the line (a) (Fig. 1) ion pairs. One thus may also exclude ICD of $Ar^+(3p^{-2},n\ell)$-Ar ions as the origin of the KER line (b) ion pairs.

A DI mechanism that may be responsible for the line (b) ion pairs, which moreover is compatible with the photoelectron kinetic energy distribution [27], is two-site double ionization of the dimer completely analogous to the mechanism that is responsible for line (a). However, now the double ionization is followed by a laser-induced charge transfer between the two singly ionized atomic ions at R_{eq}. This simply means that the high intensity laser pulse excites the dimer ion from the ground state to the first excited electronic state. The charge transfer results in the one-site doubly ionized

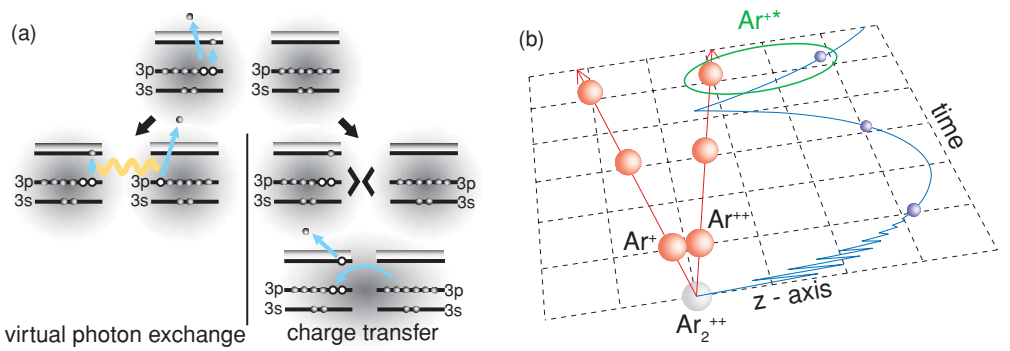

FIG. 5. (Color online) (a) Scheme of the two possible interatomic Coulombic decay pathways of excited Ar_2^{+*} dimer ions. Left-hand side, ICD via virtual photon exchange; right-hand side, ICD via charge transfer at small internuclear separation. (b) Illustration of frustrated triple ionization of Ar_2. For details see the text.

configuration $Ar^{2+}(3p^{-2})$-Ar, where the Ar atom is in the electronic ground state. The corresponding excited electronic states of the dimer have an attractive potential energy curve for nuclear motion (see the discussion above in this Sec. III B and Fig. 4). From these states it is possible for the dimer ion to decay to the two-site ionized configuration only via emission of a photon [24,28]. Compared to their radiation lifetime nuclear dynamics in the one-site doubly ionized electronic states is fast, thus allowing a closer approach of the nuclei accompanied by a corresponding higher KER after radiative reverse charge transfer and subsequent Coulomb explosion. The probability for spontaneous radiative charge transfer is expected to be highest for small internuclear separation. There the corresponding dipole matrix element, which governs the transition between the two electronic states, is expected to have a maximum since the overlap of the involved electron orbitals is maximum. One thus would expect to find a pronounced kinetic energy release in the Coulomb explosion where we find the line (b) in the spectrum.

We want to discuss the feasibility of the laser-induced charge transfer mechanism in more detail for a model doubly charged dimer with only one electron. It is assumed to consist of a doubly charged atomic ion core and a singly charged one. To this system an electron is attached. For an internuclear separation **R** the potential energy for the electron motion at fixed **R** is then given by

$$V(\mathbf{x}) = -2/|\mathbf{x} - \mathbf{R}/2| - 1/|\mathbf{x} + \mathbf{R}/2|. \quad (1)$$

We show this potential for $R_{eq} = 7.13$ a.u. in Fig. 6 [solid (red) line] along the internuclear axis (z axis). Also indicated

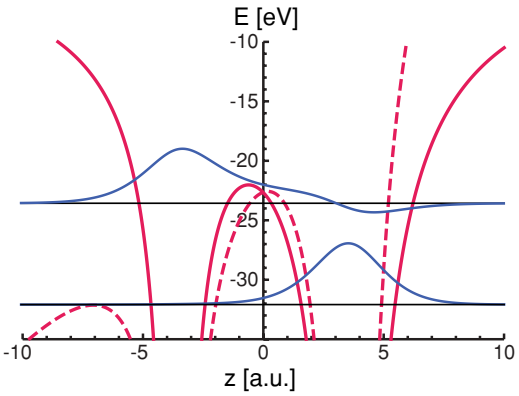

FIG. 6. (Color online) Potential energy curves $(-1/|z + R_{eq}/2| - 2/|z - R_{eq}/2|)$ for electron motion along the internuclear axis in a model Ar_2^{2+} dimer ion plotted for an internuclear separation $R = R_{eq}$ [solid (red) line]. The dashed (red) line indicates the same potential as before, however, now superimposed with the potential of a homogeneous external electric field. The external field strength is chosen to be equal to the peak laser pulse field strength of 0.1 a.u. in the experiment. The two horizontal lines represent the two lowest lying electronic energy eigenvalues of Ar_2^{2+} (from [15]). Superimposed on these lines, we show the corresponding electronic wave functions we derived for a one-dimensional model Ar_2^{2+} dimer. In the ground state the electron is localized at the Ar_2^{2+} site. As can be seen the first excited state is the charge transfer state where the electron is mainly localized at the Ar^+ site. The zero point of the energy scale corresponds to removal of the electron to infinity with the two nuclei fixed at R_{eq}.

in this figure are the electronic energy eigenvalues at $R_{eq} = 7.13$ a.u. for the Ar_2^{2+} electronic states that correspond to the configurations $Ar^+(3p^{-1})$-$Ar^+(3p^{-1})$ (a mean energy value is used here, since several closely spaced electronic states correspond to this configuration) and to $Ar^{2+}(3p^{-2})$-Ar (the energy eigenvalue for the state that dissociates into the atomic ground states $Ar^{2+}(3p^{-2})\ ^3P$ and Ar ^1S is used). The eigenvalues have been derived from the potential energy curves given in [15]. The energy eigenvalue for the ground state is well below the central Coulomb barrier of the potential at $z = 0$ while that of the first excited state, the charge transfer state, is only slightly below the top of this barrier. The energy difference between these states is ≈8.4 eV. Together with the energy eigenvalues, we indicated in the figure the electronic wave functions that we have derived from a one-dimensional model for this system. This model is based on a "soft" Coulomb potential with the potential energy along the internuclear axis (z axis) given by

$$V(z) = -2/\sqrt{(z - R/2)^2 + a^2} - 1/\sqrt{(z + R/2)^2 + b^2}. \quad (2)$$

We adjusted the "softening" parameters a and b so as to reproduce the Ar_2^{2+} electronic energy eigenvalues from [15] in Fig. 6. For the ground state the model wave function is completely localized on the doubly charged ion core. This means the dimer is two-site singly ionized. However, in the excited charge transfer state the electron is no more strictly localized on the singly charged ion core to neutralize its positive charge completely. The already small central potential barrier allows some leakage to the other side.

Using the dipole approximation and the length gauge the time-dependent interaction of the model dimer electron with the external laser pulse is represented by a time-dependent potential $V_I(x,t)$. If we assume the internuclear axis to be aligned along the laser pulse polarization direction it reads

$$V_I(z,t) = -F_0(t)\, z\, \cos(\omega t + \phi),$$

with $F_0(t)$ being the amplitude of the laser pulse electric field, ω the laser pulse central frequency, and ϕ the carrier-envelope phase. Superimposing $V_I(z,t)$ on the internal potential energy $V(z)$ gives rise to the potential energy curve represented by the dashed (red) line in Fig. 6. Here, the experimentally reached electric-field strength maximum of the laser pulse of $F_0 = 0.1$ a.u. was assumed with the polarization vector pointing along the internuclear axis. The curve corresponds to the electric-field vector pointing to the right. It is obvious that the internal dimer potential at the levels of the energy eigenvalues becomes strongly distorted in the external field. The unperturbed excited dimer state is even no longer bound. It is prone to above-barrier ionization close to the pulsed field strength maximum. The same is true for the ground state when the external electric field reverses sign. If one assumes that Ar_2^{2+} is formed in the electronic ground state after strong-field double ionization of Ar_2 the significantly distorted potential that governs the electron motion in the laser pulse drives an electronic wave packet. At the end of the pulse there will then certainly remain a nonzero probability to find the system in the excited electronic state where the electron is transferred to the singly charged ion core site in the dimer.

We checked the feasibility of laser-induced charge transfer in the Ar_2^{2+} dimer ion under our experimental conditions by solving the time-dependent Schrödinger equation for the previously introduced one-dimensional model dimer with a laser pulse applied. We started the calculation assuming that initially the model Ar_2^{2+} dimer is in the ground two-site ionized electronic state (see Fig. 6) where the electron is located at the doubly charged ion core site. Then we apply the full laser pulse and calculate the time evolution of the wave packet up to the end of the pulse. We used a 10-cycle pulse for the calculation with a peak electric-field strength reaching 0.075 a.u. This corresponds to a peak intensity of $2 \times 10^{14}\,\mathrm{W/cm^2}$. The electric-field amplitude function was chosen to be $F_0(t) = F_0 \sin^2(\omega t/2n)$ in the time interval $[0,nT]$ with n being the number of optical cycles of the pulse. T is the width of one optical cycle of the pulse and $\omega = 2\pi/T$ the frequency of the carrier wave. The pulse width chosen is approximately half of the experimental pulse width.

For each time step of the integration the exact propagator for the time-dependent Schrödinger equation is approximated by $\exp[-i\int_t^{t+\Delta t} dt' H(t')]$, that is, by the lowest order term of its Magnus expansion [29]. In order to evaluate this approximate propagator numerically we used the split operator technique [30] by splitting $H(t)$ into its kinetic energy part T_R and the time-dependent potential $V(z,t)$ which consists of the Coulomb interaction of the electron with the two nuclei and and its interaction with the external time-dependent electric field. The approximate propagator for each time step we evaluated numerically then reads

$$\exp\left[-\frac{i}{2}\int_t^{t+\Delta t} dt' V(z,t')\right] \exp(-iT_R\Delta t) \times \exp\left[-\frac{i}{2}\int_t^{t+\Delta t} dt' V(z,t')\right].$$

The numerical procedure involves fast Fourier transforms to switch between position and momentum space. Since the integration is limited to a finite interval in position space we had to take care to avoid reflections from the spatial boundaries. This was done by introducing an additional imaginary potential in position space close to the boundaries which efficiently absorbed outgoing waves. The absorptive potential started to rise at $z = \pm 165$ a.u. toward the boundaries which were located at $z = \pm 300$ a.u.

The calculated temporal evolution of the initial electronic wave function (the two-site ionized electronic ground state of the model dimer) is shown in Fig. 7. In the figure the probability distribution $|\psi(z,t)|^2$ corresponding to the wave function $\psi(z,t)$ at times t is plotted. Time evolves along the vertical axis. It is given in multiples of the laser period T. The inserted curves shows the probability distributions for the electronic ground state (the initial, two-site ionized, state; right-hand maximum) and for the charge transfer state (the first excited, one-site ionized, eigenstate of the model dimer; left-hand main maximum). One can easily see that excitation of the dimer by the laser pulse starts with a charge transfer at $t \approx 2.5T$ already on the rising edge of the pulse. There a significant probability builds up at the position where the main maximum of the charge transfer, excited state is located. Further excitation and ionization of the dimer seems to proceed

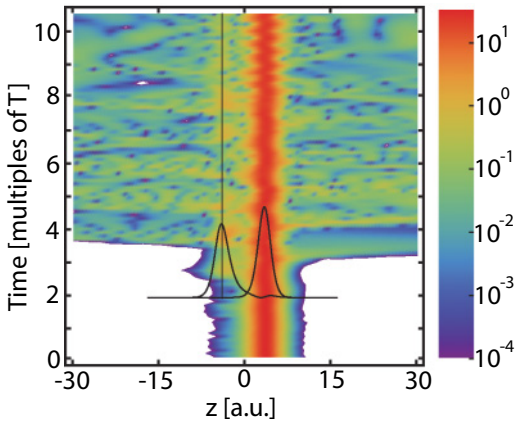

FIG. 7. (Color) Evolution in time of the electronic wave function of the initially two-site ionized model Ar_2 dimer with an external 10-cycle laser pulse applied which has a peak electric-field strength of 0.075 a.u. On a logarithmic color scale we show a density plot of the wave packet probability distribution $|\psi(z,t)|^2$. Time evolves along the vertical axis. It is given in multiples of the laser light period $T = 2.67$ fs. The inserted curves shows the absolute square of the two-site (right-hand maximum) and of the one-site (left-hand main maximum) ionized electronic eigenstates of the model atom. For further details see the text.

mainly via this state. A certain small fraction of population remains in this state up to the end of the pulse (see the evolution of the probability distribution along the vertical line in Fig. 7). At the end of the pulse the probability to find the dimer in the excited charge transfer state is ≈0.001 for the specific choice of laser pulse parameters. This value depends on the laser pulse peak intensity. It is determined by the balance between excitation from the ground state and ionization of the excited charge transfer state. Actually, we also find in the experiment significant triple ionization of Ar_2 (see Sec. III C below and Fig. 8).

Our simple approach, however, is not able to account completely for the experimental situation. There Ar_2^{2+} is

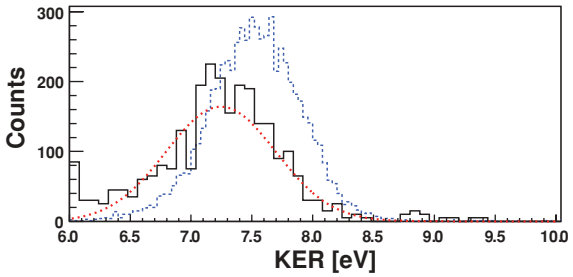

FIG. 8. (Color online) KER distribution for the Coulomb explosion channel $Ar^{2+} + Ar^{+}$ after triple ionization of the Ar_2 dimer [dashed (blue) line]. The spectrum was taken simultaneously with the corresponding KER spectrum for the Coulomb explosion channel $Ar^{+} + Ar^{+}$ in Fig. 1 with the laser beam having linear polarization. On the vertical axis the number of ion pair events per energy bin is given. Also shown is the vertically scaled high-energy part of the KER spectrum in Fig. 1 taken with linear polarization [solid (black) line]. The dotted (red) line line is a fit to the measured KER line (c) of Fig. 1 assuming that it originates from frustrated triple ionization of Ar_2. For details see the text.

formed close to the center of the light pulse where the electric-strength is high. In the model it does not make sense to start the calculation at the pulse center with the electron in the ground state since already while the two photoelectrons are leaving the dimer the third active electron (which is involved in the charge transfer) is expected to react to the applied laser pulse and is probably not in the unperturbed Ar_2^{2+} ground state. Under these conditions an initial wave function with which to start the model propagation cannot unambiguously be specified. Therefore, we have chosen to start the time evolution in the model Ar_2^{2+} ground state at the start of the light pulse and have used a pulse with approximately half of the experimental pulse width. Nevertheless, the result found for our simplified model system indicates that laser-induced charge transfer in the two-site ionized Ar_2 dimer $[Ar^+(3p^{-1})\text{-}Ar^+(3p^{-1})]$ is a feasible mechanism of formation of $Ar^{2+}(3p^{-2})$-Ar which then can give rise to line (b) in the KER spectrum via reverse radiative charge transfer at small internuclear separation.

C. Frustrated triple ionization of Ar_2 [line (c)]

The high-energy KER line (c) in Fig. 1 cannot be sensibly understood in terms of radiative charge transfer in Ar_2^{2+} at short internuclear separation. The high KER of 7.3 eV would imply that the Coulomb explosion starts at an internuclear separation of ≈3.7 a.u. However, from the literature no attractive potential energy curve of an excited Ar_2^+ or Ar_2^{2+} state is known that would allow for such a close approach of the nuclei provided that they start their motion at R_{eq} with the only few meV kinetic energy that they have after strong-field ionization of Ar_2 (Franck-Condon principle assumed).

A reasonable mechanism of formation of the weak KER line (c) in Fig. 1 can be found by looking at the triple-ionization channel of the dimer where one atom is doubly and the second one singly ionized $[Ar^{2+}(3p^{-2})\text{-}Ar^+(3p^{-1})]$. Ar_2^{3+} Coulomb explodes with a kinetic energy release of $2/R_{eq} = 0.28$ a.u. $\widehat{=}$ 7.6 eV. The corresponding KER spectrum is shown in Fig. 8 [dashed (blue) line] for linear polarization of the laser radiation. For comparison we also show the high-energy part [line (c)] of the Ar_2 double-ionization KER spectrum recorded with linearly polarized light [solid (black) line in Figs. 1 and 8]. It appears close to the KER line for Coulomb explosion of Ar_2^{3+} at R_{eq}, being only slightly displaced to lower kinetic energy. The close vicinity of these lines as well as the facts that line (c) is much weaker than the Ar_2^{3+} Coulomb explosion line and that it disappears completely for circular polarization of the laser beam is reminiscent of frustrated double ionization found in the H_2 molecule [11].

Frustrated strong-field ionization means that after electric-field ionization the electron does not gain enough drift energy in the high-intensity light pulse toward the end of the pulse to overcome the Coulomb attraction of the nucleus [10]. This happens to electrons that become field ionized close to the extrema of the electric-field strength in each oscillation period. In order to get trapped on the nucleus after the pulse is gone, the electron has to be in the vicinity of the nucleus at the end of the pulse to ensure that the Coulomb potential energy is able to compensate the gained drift kinetic energy. Moreover, the final drift kinetic energy has to be small. This is only possible for a linearly polarized laser beam. For circular polarization the drift energy E_{drift} of the electron at the end of the pulse is independent of the instant of time of electric-field ionization and always large ($E_{drift} = F_0^2/2\omega^2$, with F_0 being the electric-field strength in the laser pulse and ω the laser frequency). In this case the Coulomb interaction is not able to trap the electron at the end of the pulse. This results in a nonappearance of frustrated field ionization for circular polarization similar to nonsequential double ionization or high-order harmonic generation [10]. The electron is trapped in a broad distribution of Rydberg states with a maximum at a principal quantum number $n \approx 9$ (He, [10]). The "radius" r of Ar_2^{2+*} Rydberg orbits with principal quantum number $n \geqslant 9$ is at least $r \approx 3n^2/2Z \approx 40$ a.u. (Z is the ion core charge state; low angular momentum states assumed). This is substantially larger than the equilibrium internuclear separation $R_{eq} = 7.13$ a.u. of the Ar_2 dimer, which is fixed while the laser pulse is applied.

Frustrated triple ionization of the dimer thus means that one of the laser-excited electrons gets trapped in a Rydberg state of the Ar_2^{3+} ion core after the laser pulse is gone. Since the radius of the Rydberg orbit where the electron gets trapped is usually larger than R_{eq} (see the previous paragraph and [10]), the electron is not localized at one of the atomic ions, Ar^+ or Ar^{2+}, that form the dimer ion core. This means that, directly after the laser pulse, the two nuclei feel the full Coulomb repulsion between a doubly and singly charged Ar ion. After the internuclear separation has increased close to and then beyond the Rydberg orbit radius, the electron will get localized on one of the nuclei. In the experiment we only detected the channel where the electron gets localized on the Ar^{2+} constituent. We are presently not able to detect the second possible channel where the electron neutralizes the Ar^+ ion because of the weakness that the $Ar^{+*} + Ar^+$ dissociation channel already shows. After the electron is localized on the Ar^{2+} ion core, the Coulomb repulsion is reduced to the repulsion between two singly charged Ar ions.

We use this switching in the Coulomb repulsion as a simple test of whether this scenario makes sense as the origin of the fast KER line (c) (see Figs. 1 and 8). We start from the realistic assumption that the Coulomb explosion starts with zero initial nuclear velocity directly after the laser pulse at R_{eq}. The effective repulsive Coulomb potential is then $V(R) = 2/R$ until an internuclear separation R_1 is reached, where we assume the Rydberg electron gets localized instantaneously at the Ar^{2+} ion and shields its charge. For $R > R_1$ we assume the Coulomb potential to be reduced to $V(R) = 1/R$ for the final part of the nuclear motion. Provided that the initial distribution $f(R)$ of internuclear separations after laser excitation of Ar_2 is known and that a probability $w(R)$ for localization of the electron on the Ar^{2+} ion at an internuclear separation R is given, it is possible to establish a relation between the final KER distribution $g(E)$ of the $Ar^+ + Ar^{+*}$ ion pair and $f(R)$:

$$g(E) = 2\int_{1/E}^{\infty} dR_1 w(R_1) \frac{f[2/(E + 1/R_1)]}{(E + 1/R_1)^2}. \qquad (3)$$

The lower limit of the integral is determined by the condition that R_1 be larger than R. It is not possible to determine $w(R)$ from this relation, provided only $g(E)$ and $f(R)$ are known.

We thus assume $w(R)$ to be a Gaussian distribution:

$$w(R) = \exp\left(-\frac{(R-R_0)^2}{(\delta R)^2}\right), \quad (4)$$

with a width δR centered at R_0. This is an arbitrary choice since we do not know the correct functional form. It is meant to be a tool to get an estimate for the mean internuclear separation where the electron gets localized at the Ar^{2+} ion. We optimize δR and R_0 to fit $g(E)$ calculated from Eq. (3) to the measured KER distribution of line (c) in Fig. 8. The best fit, with $R_0 =$ 115 a.u. and $\delta R = 80$ a.u., is shown in Fig. 8 [dotted (red) line]. This simple choice of $w(R)$ already resulted in a very good fit to the shape of the experimental KER line (c). A good estimate for $f(R)$, which has to be plugged into Eq. (3), was derived from the two-site DI KER line (a) in Fig. 1. The result obtained for R_0 means that on average the electron becomes localized when the internuclear separation reaches ≈115 a.u. This choice of R_0 centers the calculated KER distribution on the measured one. This allows for an estimate of the mean principal quantum number of the Rydberg states of Ar_2^{2+} where the electron gets trapped after the laser pulse is gone. The mean radius of the Rydberg orbit has to be less than ≈115 a.u. The mean principal quantum number is therefore $n \approx 15$ (assuming small angular momentum and the relation $r \approx 3n^2/2Z$ between the mean Rydberg orbit radius and the principal quantum number). This is just in the range of principal quantum numbers where most electrons get trapped after frustrated tunnel ionization of He [10]. This result together with the disappearance of line (c) for circular light polarization is strong evidence that frustrated triple ionization is actually responsible for the KER line (c).

IV. CONCLUSION

Concluding, our experimental results indicate that strong-field excitation of the argon dimer follows several routes and triggers a variety of decay mechanisms which terminate in double ionization accompanied by Coulomb explosion. An intricate electron dynamics is involved during and after laser excitation. Strong-field excitation mechanisms compatible with our data are basic two-site electric-field ionization, which terminates in Ar_2^{2+} in the ground electronic state; double ionization accompanied by a laser-induced charge transfer in Ar_2^{2+}; and electron trapping in Rydberg states after frustrated triple ionization. The frustrated triple ionization found here is similar to the frustrated double ionization we recently observed in the hydrogen molecule [11]. The laser-induced charge transfer in Ar_2^{2+}, which neutralizes one of the ions, is reversed long after the laser pulse is gone by a spontaneous radiative reverse charge transfer, preferentially at small internuclear separation. The reverse transfer singly charges both dimer sites again and terminates in a Coulomb explosion.

Despite the only weak polarization forces that bind the neutral Ar_2 dimer, its strong-field excitation and multiple ionization are considerably influenced by the molecular structure of the system. Already the first ionization step of one of its constituent atoms creates an ion sitting close to an atom. The ion's Coulomb electric field then, for example, assists further ionization by the strong external electric field of the laser pulse. This certainly causes nonsequential double ionization, which prevails for double ionization of the Ar atom at the light intensity we used, to be of minor importance for the dimer. The data even indicate that one-site double ionization, which, at first sight, one would expect should follow a nonsequential pathway just as in the atom, happens predominantly sequentially. We expect that the DI mechanisms we found for Ar_2 are universal for molecules at large internuclear separation, where the valence electrons get localized at the atomic sites.

ACKNOWLEDGMENT

We thank the German Bundesministrium für Bildung und Forschung (BMBF) for financial support for the detector development under Contract No. 05KS4RFA/3.

[1] L. S. Cederbaum and J. Zobeley, Chem. Phys. Lett. **307**, 205 (1999).
[2] L. Lehr, T. Horneff, R. Weinkauf, and E. W. Schlag, J. Phys. Chem. A **109**, 8074 (2005).
[3] S. Lünnemann, A. I. Kuleff, and L. S. Cederbaum, Chem. Phys. Lett. **450**, 232 (2008).
[4] L. Poisson, K. D. Raffael, M.-A. Gaveau, B. Soep, J.-M. Mestdagh, J. Caillat, R. Taïeb, and A. Maquet, Phys. Rev. Lett. **99**, 103401 (2007).
[5] S. Minemoto and H. Sakai, Phys. Rev. A **75**, 033413 (2007).
[6] L. S. Cederbaum, J. Zobeley, and F. Tarantelli, Phys. Rev. Lett. **79**, 4778 (1997).
[7] T. Jahnke *et al.*, Phys. Rev. Lett. **93**, 163401 (2004).
[8] P. Lablanquie, T. Ato, Y. Hikosaka, Y. Morioka, F. Penent, and K. Ito, J. Chem. Phys. **127**, 154323 (2007).
[9] T. Jahnke *et al.*, Phys. Rev. Lett. **99**, 153401 (2007).
[10] T. Nubbemeyer, K. Gorling, A. Saenz, U. Eichmann, and W. Sandner, Phys. Rev. Lett. **101**, 233001 (2008).
[11] B. Manschwetus, T. Nubbemeyer, K. Gorling, G. Steinmeyer, U. Eichmann, H. Rottke, and W. Sandner, Phys. Rev. Lett. **102**, 113002 (2009).
[12] J. Ullrich, R. Moshammer, A. Dorn, R. Dörner, L. P. H. Schmidt, and H. Schmidt-Böcking, Rep. Prog. Phys. **66**, 1463 (2003).
[13] Z. Ansari, M. Böttcher, B. Manschwetus, H. Rottke, W. Sandner, A. Verhoef, M. Lezius, G. G. Paulus, A. Saenz, and D. B. Milošević, New J. Phys. **10**, 093027 (2008).
[14] P. Slavícek, R. Kalus, P. Paska, I. Odvárková, P. Hobza, and A. Malievský, J. Chem. Phys. **119**, 2102 (2003).
[15] C. Cachoncinlle, J. M. Pouvesle, G. Durand, and F. Spiegelmann, J. Chem. Phys. **96**, 6085 (1992).
[16] T. Weber *et al.*, Phys. Rev. Lett. **84**, 443 (2000).
[17] R. Moshammer *et al.*, Phys. Rev. Lett. **84**, 447 (2000).
[18] P. Dietrich, N. H. Burnett, M. Ivanov, and P. B. Corkum, Phys. Rev. A **50**, R3585 (1994).
[19] T. Seideman, M. Y. Ivanov, and P. B. Corkum, Phys. Rev. Lett. **75**, 2819 (1995).
[20] J. Posthumus, L. J. Frasinski, A. J. Giles, and K. Codling, J. Phys. B **28**, L349 (1995).
[21] S. Chelkowski and A. D. Bandrauk, J. Phys. B **28**, L723 (1995).
[22] W. R. Wadt, J. Chem. Phys. **68**, 402 (1978).
[23] C. Cachoncinlle, J. M. Pouvesle, G. Durand, and F. Spiegelmann, J. Chem. Phys. **96**, 6093 (1992).

[24] S. D. Stoychev, A. I. Kuleff, F. Tarantelli, and L. S. Cederbaum, J. Chem. Phys. **128**, 014307 (2008).
[25] R. Santra and L. S. Cederbaum, Phys. Rep. **368**, 1 (2002).
[26] V. Averbukh, I. B. Müller, and L. S. Cederbaum, Phys. Rev. Lett. **93**, 263002 (2004).
[27] B. Ulrich, A. Vredenborg, A. Malakzadeh, M. Meckel, K. Cole, M. Smolarski, Z. Chang, T. Jahnke, and R. Dörner, Phys. Rev. A **82**, 013412 (2010).
[28] N. Saito, Y. Morishita, I. H. Suzuki, S. D. Stoychev, A. I. Kuleff, L. S. Cederbaum, X.-J. Liu, H. Fukuzawa, G. Prümper, and K. Ueda, Chem. Phys. Lett. **441**, 16 (2007).
[29] R. Blanes, F. Casas, J. A. Oteo, and J. Ros, J. Phys. A **31**, 259 (1998).
[30] M. D. Feit, J. J. A. Fleck, and A. Steiger, J. Comput. Phys. **47**, 412 (1982).